

The anisotropic magnetoresistance in Fe/Pt compositionally modulated films

This article has been downloaded from IOPscience. Please scroll down to see the full text article.

1994 J. Phys.: Condens. Matter 6 8187

(<http://iopscience.iop.org/0953-8984/6/40/010>)

View [the table of contents for this issue](#), or go to the [journal homepage](#) for more

Download details:

IP Address: 171.66.16.151

The article was downloaded on 12/05/2010 at 20:41

Please note that [terms and conditions apply](#).

The anisotropic magnetoresistance in Fe/Pt compositionally modulated films

C Christides†, I Panagiotopoulos†, D Niarchos†, T Tsakalakos‡ and A F Jankowski§

† Institute of Materials Science, National Centre for Scientific Research Demokritos, 153 10 Aghia Paraskevi, Attiki, Greece

‡ Department of Mechanics and Materials Science, Rutgers University, Piscataway, NJ 08855-0909, USA

§ Chemistry and Materials Science Department, Lawrence Livermore National Laboratory, PO Box 808, Livermore, CA 94550, USA

Received 6 April 1994

Abstract. The anisotropic nature of the resistivity of magnetic multilayers under a parallel or perpendicular applied magnetic field is addressed by magnetoresistivity and hysteresis loop measurements. It is shown that the observation of anisotropic magnetoresistance (AMR) at 80 K can provide straightforward information on the magnetic properties of successive layers in Fe/Pt multilayers. The relative as well as absolute Fe and Pt thicknesses are critical for the AMR behaviour. For Fe layer thicknesses t_{Fe} less than 5 Å both ρ_{\parallel} and ρ_{\perp} increase initially as a function of the applied field H while for larger t_{Fe} ρ_{\perp} always decreases. The anomalous AMR for $t_{\text{Fe}} < 5$ Å is attributed to an inclination of the Fe magnetization out of the film's plane.

1. Introduction

Metallic multilayers with perpendicular magnetic anisotropy have attracted considerable attention as alternative magneto-optic (MO) storage materials. These are Co/Pt and Co/Pd compositionally modulated multilayer films (CMFs) with nominal magnetic layer thicknesses in the 1–2 monolayer range and an overall thickness of only 20–30 nm. It is well established from band structure calculations [1], circular magnetic x-ray dichroism (CMXD) [2], x-ray photoemission (XPS) [3] and neutron [4] measurements that Pt, in Co/Pt CMFs and alloys, carries a sizeable magnetic moment (0.2–0.5 μ_{B} per Pt layer), which explains the observed UV Kerr rotation angles of up to 0.6°. There is a direct correlation of the MO–Kerr effect to electronic properties since MO effects are the result of a complicated interplay between optical and magneto-optical electronic transitions, involving spin–orbit coupling and spin polarization of the respective electronic states at the same time. The exchange polarized Pt in Co/Pt CMFs has been considered to give rise to strong Kerr rotation via excitations of the 5d band.

Recently, perpendicular magnetic anisotropy (PMA) has also been reported [5] for Fe/Pt CMFs. The magnetic properties of these films are strongly dependent on the relative as well as the absolute Fe and Pt layer thicknesses. For films grown by electron beam evaporation onto glass fused quartz and Si substrates it is found that PMA is accomplished for less than 5 Å Fe layer thickness [6]. The higher the substrate deposition temperature, the larger the intrinsic PMA constant K_{\parallel} becomes [6]. In addition, the saturation magnetization is found to exceed the value of pure Fe for temperatures lower than 180 K. CMXD measurements [7]

performed on an $(\text{Fe}_9/\text{Pt}_9)_{92}$ CMF, prepared by magnetron sputtering on Si ([111] textured in the growth direction), shows that at room temperature the magnetic moment is $\sim 1\mu_B/\text{Fe}$ and lies on the film's plane. However the value of θ_k , at room temperature, for Fe/Pt films with PMA is rather small compared to Co/Pt CMFs with almost the same Pt concentration. This difference is considered to originate from the drop in Curie temperature T_C for Fe/Pt CMFs.

In the Fe/Pt CMFs the exchange polarized Pt, associated with the observed Kerr rotation effect, must be considerably influenced by the direction of magnetization in the Fe layers. Since the thickness of the Fe layer determines the orientation of the magnetic moment relative to the surface of the film, the existence of the desirable PMA is correlated with the variation of the spin-orbit coupling and 3d band splitting in the Fe layers. The strength of these interactions is expected to affect the anisotropic magnetoresistance (AMR) [8] in these materials. This effect, found in ferromagnets, depends on the orientation of the magnetization with respect to the electric current direction in the material. In this study we present the variation of AMR together with magnetic measurements as a function of Pt and Fe thicknesses on a series of Fe/Pt CMFs.

2. Experimental details

The Fe/Pt multilayer samples were prepared by magnetron sputtering deposition in the DC mode in a cryogenically pumped chamber with a base pressure of 10^{-7} Torr. The cleaved mica substrates, positioned at 20 cm above a circular array of individually shielded sputtering sources, were sequentially rotated over each collimated target at 1 rpm. The oxygen-free Cu substrate table was maintained near room temperature ($< 40^\circ\text{C}$) during the deposition. The deposition rates were approximately 1 \AA s^{-1} for both Fe and Pt. The target materials were 0.9999% pure and 6.7×10^{-1} Pa Ar gas working pressure was used to sputter the target material. The nominal compositions of each sample was monitored with a quartz crystal calibrated at 6 MHz. The final thickness for all CMFs was between 170 and 190 nm.

AMR measurements were performed by the standard four-probe technique for DC resistivity measurements. The current and voltage leads were brought into contact with the film surface with a mechanical contact of four Cu strips on a plastic plate. A Hewlett-Packard 3478A multimeter was used to supply the DC current and measure the drop of the voltage along the film specimen. An electromagnet with a maximum homogeneous magnetic field of ± 2 T was used for the MR measurements. The magnetic measurements were performed with a Quantum Design MPMSR2 SQUID magnetometer.

The lattice and layer pair spacings of the Fe/Pt films were measured with x-ray diffraction (XRD) [9]. A detailed structural analysis of the samples by XRD and TEM will be published elsewhere. The XRD data indicate that the samples are oriented along the [111] direction of an FCC lattice. In addition, satellites up to third order were observed about (000) indicating an abrupt Fe/Pt interface with a limited Fe/Pt intermixing.

3. Experimental results

3.1. Magnetoresistance

Measurements were performed with the applied field H parallel and perpendicular to the film plane and current direction. The MR effect was negligible at room temperature for all specimens and reliable signals were obtained at 80 K. The observed ratios $\Delta\rho/\rho =$

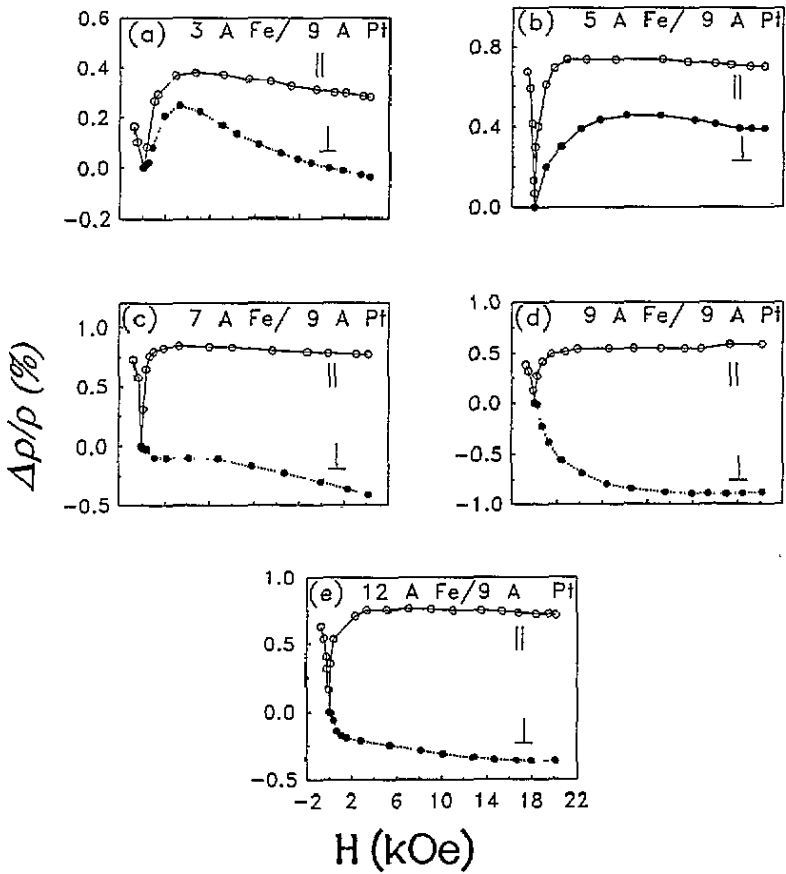


Figure 1. The ratio $\Delta\rho/\rho$ as a function of the applied field H parallel and perpendicular to the film plane for the samples with constant $t_{Pt} = 9 \text{ \AA}$ and $t_{Fe} = 3, 5, 7, 9,$ and 12 \AA .

$R(H) - R(0)/R(0)$ for the parallel and perpendicular directions are illustrated in figures 1 and 2. The experimental points in figures 1 and 2 were taken with the applied field initially increased from zero to saturation and then reduced to a small reverse field during the measurements. All the films with Fe layer thicknesses $t_{Fe} > 5 \text{ \AA}$ demonstrate a typical AMR behaviour [8]. The non-magnetized films are in a multidomain magnetic configuration. The initial increase (decrease) of $\rho_{\parallel}(\rho_{\perp})$ is attributed to the alignment of the magnetization parallel to the applied field direction. The arrows in figure 2 mark the selection of resistivity values to determine the AMR associated with the orientation of the spontaneous moment M_s . The normalized quantity

$$\langle \text{AMR} \rangle = (\rho_{\parallel} - \rho_{\perp}) / (\frac{1}{3}\rho_{\parallel} + \frac{2}{3}\rho_{\perp}) \quad (1)$$

is called the anisotropic resistivity ratio and can be obtained directly from $\Delta R/R$ without the need to know the dimensions of the specimen. The field was applied parallel to the film plane and perpendicular or parallel to the current direction as well in order to investigate the effect of the in plane anisotropy on MR measurements. In both cases the observed MR against H curves gave the same results within experimental error. This implies that the in plane anisotropy or texture of the polycrystalline CMFs is not enough to contribute

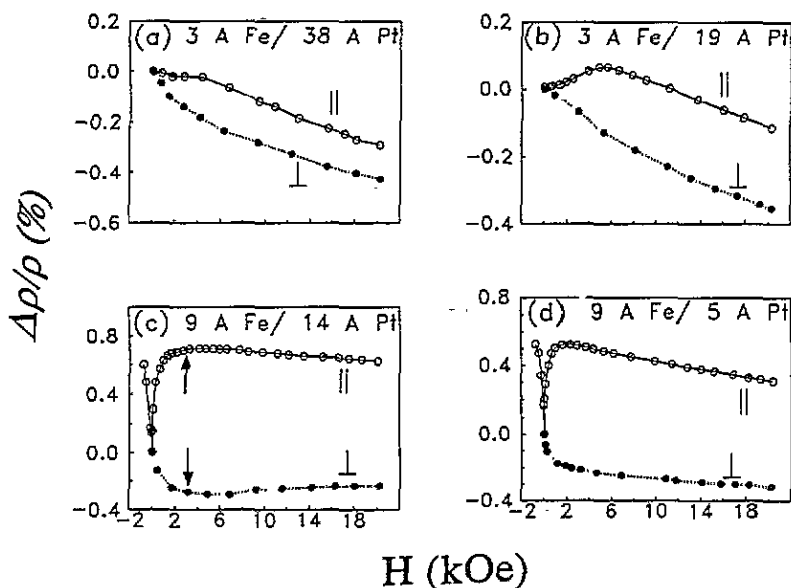


Figure 2. The ratio $\Delta\rho/\rho$ as a function of the applied field H parallel and perpendicular to the film plane for the samples with $t_{\text{Fe}} = 3 \text{ \AA}$, $t_{\text{Pt}} = 19$ and 38 \AA and $t_{\text{Fe}} = 9 \text{ \AA}$, $t_{\text{Pt}} = 14$ and 5 \AA .

Table 1. Estimated values for AMR at 80 K.

t_{Fe} (\AA)	t_{Pt} (\AA)	$\langle \text{AMR} \rangle$
9	14	0.86
9	9	1.47
9	5	0.63
7	9	1.29
12	9	0.63

macroscopically to the observed $\langle \text{AMR} \rangle$ in these samples. The extracted $\langle \text{AMR} \rangle$ values for the specimens with $t_{\text{Fe}} > 5 \text{ \AA}$ are listed in table 1.

There are three sets of specimens related to the thickness of Fe and Pt layers. The first category consists of specimens with constant $t_{\text{Pt}} = 9 \text{ \AA}$ and varying $t_{\text{Fe}} = 3, 5, 7, 9$, and 12 \AA . The purpose of this systematic variation of Fe thickness was to study the MR effect of the reported [5, 6] PMA in the Fe/Pt system. As shown in figure 1, the $t_{\text{Fe}} = 3$ and 5 \AA CMFs clearly demonstrate a deviation of the typical AMR behaviour since both $\Delta\rho_{\parallel}$ and $\Delta\rho_{\perp}$ versus H show an initial increase. This effect is almost visible for specimen $t_{\text{Fe}} = 7 \text{ \AA}$ and totally disappears for $t_{\text{Fe}} = 9$ and 12 \AA .

In the second and third set of Fe/Pt CMFs, the Fe thickness is fixed at 3 and 9 \AA respectively whereas t_{Pt} is varied. The MR behaviour in the second and third set of Fe/Pt films is depicted in figure 2 and must be considered complementary to figure 1(a) and (c). For the films $\text{Fe}_3/\text{Pt}_{19}$ and $\text{Fe}_3/\text{Pt}_{38}$ the field dependence of the resistivity is closer to a 'spin valve' type of MR behaviour [10], which is always characterized by an initial decrease of the MR for an increasing magnetic field. In the $t_{\text{Pt}} = 38 \text{ \AA}$ film this MR effect is more pronounced and seems to degrade progressively for smaller $t_{\text{Pt}} = 19$ and 9 \AA in the specimens with fixed $t_{\text{Fe}} = 3 \text{ \AA}$, to a rather anomalous AMR behaviour. On the third series of Fe/Pt CMFs, with constant $t_{\text{Fe}} = 9 \text{ \AA}$ and $t_{\text{Pt}} = 5, 9$ and 14 \AA , a typical [8] AMR behaviour

is observed for all of them. It is worth noting that the $\langle \text{AMR} \rangle$ presents a maximum, as a function of the Pt thickness in the third set, for $t_{\text{Pt}} = 9 \text{ \AA}$ (see table 1).

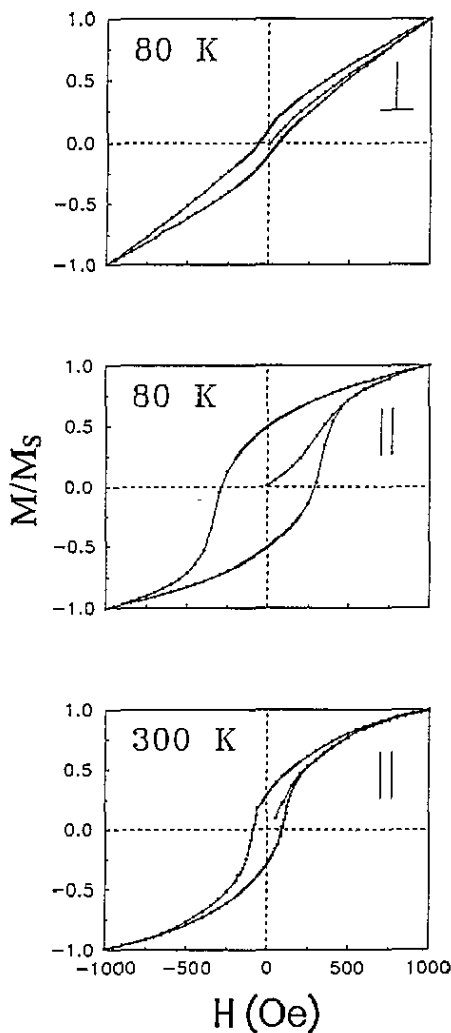


Figure 3. Hysteresis loops of the film with $t_{\text{Fe}} = 3 \text{ \AA}$, $t_{\text{Pt}} = 9 \text{ \AA}$ measured at 80 K with the applied field perpendicular and parallel to the film plane and at 300 K with the applied field parallel to the film plane.

3.2. Magnetic measurements

The observed magnetic hysteresis ($M-H$) loops for the specimen Fe_3/Pt_9 obtained with the plane of the film parallel (in plane) or perpendicular to the field direction, are shown in figure 3. The following are obvious from the loop shapes.

(i) The lack of 'squareness' in the parallel configuration at 80 and 300 K is indicative of an inclination of the averaged 'easy axis' magnetization direction out of the film's

plane. This interpretation is in agreement with the conversion electron ^{57}Fe Mössbauer spectroscopy (CMS) [9] experiments, performed in all the specimens examined here at ambient temperature. The CEMS results indicate that for $t_{\text{Fe}} < 5 \text{ \AA}$ and $t_{\text{Pt}} = 9 \text{ \AA}$ there is a non-zero magnetic component perpendicular to the film plane, whereas for $t_{\text{Fe}} > 5 \text{ \AA}$ the Fe moment lies in the plane. Furthermore, a recent work with ^{57}Fe transmission Mössbauer spectroscopy [11] has shown an inclination angle of $\sim 60^\circ$ of the magnetic moment out of the film plane at 4.2 K in Pt(20 \AA)/Fe(2 \AA) films, which demonstrates clearly that the magnetic anisotropy for $t_{\text{Fe}} < 5 \text{ \AA}$ favours a PMA at low temperatures as well.

(ii) The perpendicular $M-H$ loop at 80 K, which presents smaller coercivity H_c , shows that the 'easy axis' is closer to the film plane than to the perpendicular direction.

(iii) There is a considerable reduction of the $M-H$ loop at 300 K, indicating a significant depression of the magnetization at that temperature. This is consistent with the negligible MR observed in room temperature measurements. Since the magnetization data in figure 3 have been normalized to the maximum field value for clarity, it is worth noting that the magnetization at 300 K for $H_{\parallel} = 1000 \text{ Oe}$ is reduced to $\sim \frac{2}{3}$ of the corresponding value at 80 K.

The $M-H$ loops for the $\text{Fe}_9/\text{Pt}_{14}$ and Fe_9/Pt_5 CMFS at 80 K are shown in figure 4. These specimens have a loop shape that indicates that the interlayer magnetic coupling is ferromagnetic. Furthermore, H_c decreases for smaller Pt thicknesses in the series with fixed $t_{\text{Fe}} = 9 \text{ \AA}$.

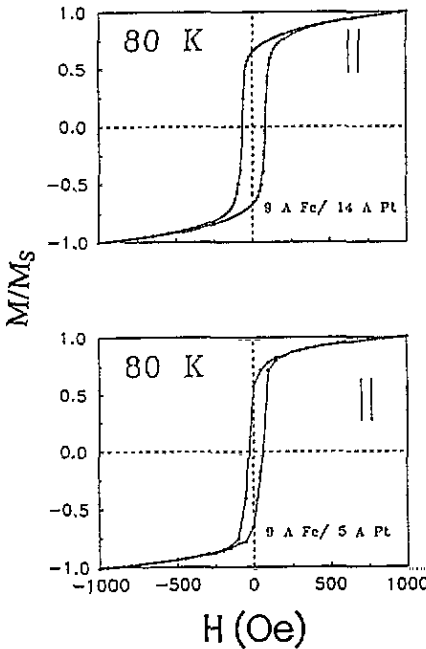


Figure 4. Hysteresis loops of the films with $t_{\text{Fe}} = 9 \text{ \AA}$, $t_{\text{Pt}} = 14 \text{ \AA}$ and $t_{\text{Fe}} = 9 \text{ \AA}$, $t_{\text{Pt}} = 5 \text{ \AA}$ measured at 80 K with the applied field parallel to the film plane.

4. Discussion

The existence of detectable AMR in CMF specimens has been proved to be a simple experimental method that can provide, in general, useful information about the magnetic properties of multilayered films. In particular, it has been shown that the existence of AMR in Fe/Pt CMFs indicates the following.

(i) A ferromagnetic arrangement of inter- and intra-layer magnetic moments lying in the film's plane. It is known [6–8] that for $t_{\text{Fe}} > 5 \text{ \AA}$ in Fe/Pt CMFs the magnetization of Fe layers is parallel to the film plane. This information has been obtained in a straightforward way in the present experiment.

(ii) The sign of $\langle \text{AMR} \rangle$ determines the contribution of the majority and minority spin electrons to the conductivity. According to Potter's model [12] the condition $\rho_{\parallel} > \rho_{\perp}$ ($\rho_{\parallel} < \rho_{\perp}$) is due to the scattering of minority (majority) spin electrons. From a microscopic quantum theory point of view, the ferromagnetic resistivity anisotropy (usually called AMR) is a consequence of an isotropic scattering potential with lower than cubic symmetry wavefunctions. The symmetry of the wavefunctions is lowered by the spin-orbit interaction. Of importance in Potter's theory for $\langle \text{AMR} \rangle$ are the ratios $N_s(E_F)/N_d(E_F)$, λ/ε and $\lambda/2\gamma$, where $N_i(E_F)$ is the electronic density of states at the Fermi level, λ is the spin-orbit coupling parameter ($H_{\text{so}} = \lambda LS$), ε is the splitting between the uppermost two d bands of like spin and 2γ is the exchange splitting constant. The N_s/N_d ratio gives the relative importance of anisotropic ss scattering and anisotropic sd scattering. A small value of ε tends to make $\langle \text{AMR} \rangle$ large and positive while a small 2γ tends to make $\langle \text{AMR} \rangle$ large and negative. In Potter's theory there is a competition between these effects and the sign of AMR depends on the details of the bands and the location of the Fermi level. In addition, it has been shown [13] that the presence of a virtual bound state at the minority spin Fermi surface, in bulk Ni alloys containing transition metal (TM) impurities, can also affect the sign of the AMR via an $L_z S_z$ spin-orbit mechanism. Thus the existence of a positive AMR cannot justify in general the claim for large spin-orbit coupling in 3d TM alloys containing other TM impurities. However, the $L_z S_z$ spin-orbit mechanism is based on Friedel's d resonant state model [14] extended by Kanamori [15], where the band structure is greatly simplified, and has been used [13] as a good approximation to explain in particular the oscillatory behaviour in the sign of $\langle \text{AMR} \rangle$ for third-series TM impurities in Ni. Therefore, the simplifications involved in this $L_z S_z$ scattering mechanism first, makes questionable its application for other 3d-TM based alloys; second, it is completely unreliable for two-dimensional CMF materials. On the other hand, Potter's model is a realistic band structure extension of the basic model of Smit [16], which calculates analytically the resistance anisotropy for FCC single crystal alloys of Ni and Cu. In this calculation the Fermi level is assumed to lie near the top of uniformly exchange split d bands. If this assumption is valid in some other ferromagnetic TM alloys or multilayered films then Potter's conclusions can be used as a first approximation to explain the AMR effect on these systems. An outline of his results can be given as follows. (a) It is shown that AMR with $\rho_{\parallel} > \rho_{\perp}$ results from sd scattering of *minority spin* electrons only and the *majority spin* current drives $\langle \text{AMR} \rangle$ negative. Moreover, energy separations between sheets of the Fermi surface of predominantly the *same* spin are more important in producing the condition $\rho_{\parallel} > \rho_{\perp}$ than are exchange splittings. (b) The spin-orbit interaction causes an anisotropy in the scattering of minority spin electrons and allows majority spin electrons to scatter into d states.

The Fe/Pt interfaces of the thinner Fe monolayers were observed with EXAFS measurements to be strongly modified from the Pt FCC layers into an Fe FCC-like packing. These results are to be presented in a forthcoming publication. It is a fair approximation

to assume that the Fermi energy of the Fe/Pt adjacent layers lies on the top of the exchange split Fe and Pt polarized band in order to satisfy the condition for the application of Potter's model. Since $\langle \text{AMR} \rangle$ is positive for all the Fe/Pt CMFs examined here, it is easy to conclude that the scattering is due to minority spin current. Assuming that the observation of the AMR effect is due to electronic spin scattering primarily in the Fe (ferromagnetic) layers and the Fe/Pt interfaces, then the spin-orbit interactions, which are responsible for the AMR, indicate the contribution of an orbital moment in the total moment per Fe layer. This is in agreement with a recent application of a set of sum rules in the Fe spin moment analysis of CMXD data [7] for $(\text{Fe}_9/\text{Pt}_9)_{92}$ CMFs, which gave an orbital moment of $\sim 0.08\mu_B/\text{Fe}$ and a spin moment of $\sim 0.90\mu_B/\text{Fe}$ for a total observed moment of $1\mu_B/\text{Fe}$ at room temperature. However, the AMR effect is negligible at room temperature and shows that the Fe magnetization is relatively low to initiate ferromagnetic resistivity anisotropy.

(iii) A deviation from the ordinary AMR behaviour can be correlated with an inclination of the particular crystallographic (easy axis) direction, where the magnetization is constrained from the spin-orbit coupling, out of the film's plane. For instance, in the Fe/Pt films with $t_{\text{Fe}} = 3 \text{ \AA}$ there are approximately two Fe monolayers, and their structure is expected to be strongly modulated from the FCC structure of Pt. Therefore, the distortions of the Fe crystal lattice induced by variations of the interface roughness between Pt and Fe layers, which is of the order of t_{Fe} , can be considered to be responsible for the coercivity mechanism.

It has been shown [17] that the wall pinning is a major factor for high coercivity in $\text{Co}_3/\text{Pt}_{10}$ CMFs, where with less interfacial sharpness the pinning size increases. It is suggested that the domain wall motion can be influenced by pinning sites present only in and nearby Co layers and *not* in Pt regions, because the Pt atoms can be magnetically polarized near the interface, but hardly at all inside the Pt layer. Consequently, any fluctuations around the interface, of the order of a few ångströms, should play a role as a pinning site for the wall motion. It is reasonable, as a first approximation, to use the same model as for the coercivity mechanism of Co/Pt films for the interpretation of the observed variations in H_c for different Fe and Pt layer thicknesses. According to this model the observed decrease of H_c on decreasing t_{Pt} from 14 to 5 Å, for $t_{\text{Fe}} = 3 \text{ \AA}$, can be explained from a better interface sharpness in the thinner Pt layer.

5. Summary

In summary, we have demonstrated in the Fe/Pt CMFs that the measurement of AMR in (magnetic/noble metal/magnetic) films is a simple experimental method to obtain, at the same time, information regarding the following.

(i) The interlayer magnetic coupling and the orientation of the magnetic moment. For $t_{\text{Fe}} > 5 \text{ \AA}$, in Fe/Pt, it is shown that the Fe magnetic moment lies on the film plane and there is a ferromagnetic interlayer coupling. On the other hand, CMFs with $t_{\text{Fe}} < 5 \text{ \AA}$ present a considerable deviation of ρ_{\perp} as a function of H from that expected in a typical AMR measurement. This behaviour has been associated with an 'out of plane' inclination of the Fe magnetization.

(ii) According to Potter's model the sign of $\langle \text{AMR} \rangle$ shows whether the resistivity is due to majority or minority electronic spins. Thus, the observed $\rho_{\parallel} > \rho_{\perp}$ condition in Fe/Pt CMFs might be caused by minority spin electronic scattering.

Acknowledgments

It is a pleasure to acknowledge Dr A Simopoulos, A Kostikas and E Devlin for helpful discussions. AJ and TT are indebted for support from the US Department of Energy under Lawrence Livermore National Laboratory contract No W-7405-ENG-48. The work at Demokritos was supported by the BRITE/EURAM-CT91-405 project of the EU.

References

- [1] Ebbert H, Ruegg S, Schutz G, Wienke R and Zeeper W B 1991 *J. Magn. Magn. Mater.* **93** 601
- [2] Ruegg S, Schutz G, Fischer P, Wienke R, Zeeper W B and Ebert H 1990 *J. Appl. Phys.* **69** 5655
- [3] Weller D, Reim W, Sporl K and Brandle H 1991 *J. Magn. Magn. Mater.* **93** 183
- [4] Menzinger F, and Paoletti A 1966 *Phys. Rev.* **143** 365
- [5] Katayama T, Suzuki Y, Nishihara Y, Sugimoto T and Hashimoto M 1991 *J. Appl. Phys.* **69** 5658
- [6] Iwata S, Parkin S S P, Nuri H and Suzuki T 1991 *Mater. Res. Soc. Symp. Proc.* vol 232 (Pittsburgh, PA: Materials Research Society) p 85
- [7] Waddil G D, Tobin J G, Jankowski A F 1993 *J. Appl. Phys.* **74** 6999
- [8] McGuire T R and Potter R I 1975 *IEEE Trans. Magn.* **MAG-11** 1018
- [9] Devlin E, Psycharis V, Kostikas A, Simonopoulos A, Niarchos D, Jankowski A, Tsakalakos T, Hong-Van and Hadjipanagis G 1993 *J. Magn. Magn. Mater.* **120** 236
- [10] George J M, Pereira L G, Barthelemy A, Petrof E, Steren L, Duvail J L, Fert A, Locoee R, Holody P and Schroeder P A 1994 *Phys. Rev. Lett.* **72** 408
- [11] Brand B A, von Schwartzberg Th, Bohne O and Keune W 1993 *J. Magn. Magn. Mater.* **126** 248
- [12] Potter R I 1974 *Phys. Rev. B* **10** 4626
- [13] Jaoul O, Campbell I A and Fert A 1977 *J. Magn. Magn. Mater.* **5** 23
- [14] Friedel J 1958 *Nuovo Cimento* **7** (Supplement 2) 287
- [15] Kanamori J 1965 *J. Appl. Phys.* **36** 929
- [16] Smit J 1951 *Physica* **16** 612
- [17] Suzuki T, Notarys H, Dobbertin D C, Lin C J, Weller D, Miller D C and Gorman G 1992 *IEEE Trans. Magn.* **MAG-28** 2754